Assessing impacts of future climate change on hydrological processes in an urbanizing watershed with a multimodel approach

Jian Sha, Yue Zhao, Xue Li and Zhong-liang Wang

ABSTRACT

The sensitivity of hydrological processes to the changed environment is of great concern. The integrated impacts of climate change and urbanization in the future have been assessed in a watershed in Northwest China through a multimodel approach based on the combined application of Generalized Watershed Loading Functions, the Long Ashton Research Station Weather Generator, and the Land Change Modeler. The results showed that both climate change and urbanization would lead to more watershed streamflow, and their combination would have synergistic effects on additional increases. In addition, there would be different seasonal distributions of streamflow with a greater proportion of runoff. These study results are helpful in supporting projects and/or decision-making processes for managers by providing more insights into the regional hydrological changes affected by climate change and urbanization. The proposed methodology of the combined multimodel approach may be applicable in other areas with similar conditions.

Key words | climate change, hydrological process, land use, model linkage, urbanization

Jian Sha
Xue Li
Zhong-liang Wang
Tianjin Key Laboratory of Water Resources and Environment,
Tianjin Normal University,
Tianjin 300387,
China

Yue Zhao (corresponding author)
Water Environment Institute, Chinese Academy for Environmental Planning,
Beijing 100012,
China
E-mail: *zhaoyue@caep.org.cn*

HIGHLIGHTS

- A multimodel linkage approach was proposed for future hydrological estimations.
- The individual and combined effects of climate change and urbanization were investigated.
- Both individual effects would increase streamflow and change its seasonal distribution.
- The combined effect had a synergistic mechanism for the additive increase of streamflow.
- There would be higher streamflow with more runoff and an earlier peak of snowmelt in future spring.

INTRODUCTION

Water is critical for human communities (Milly *et al.* 2008; Vorosmarty *et al.* 2010). The responses of watershed hydrological processes to the changing environment are of vital importance for regional security and sustainable development which are of great concern (Tan & Gan 2015; Wada *et al.* 2017). Regional climate change is one of the most significant natural influences on local hydrological properties (Oki & Kanae 2006; Kristvik *et al.* 2018). As the source and driving force of streamflow, precipitation is the key factor in hydrological processes. In addition, the air temperature determines the water state when it is transferred in the watershed. Given the expected changes in the climate in the future, the estimation of its impact on watershed streamflow and water balance behavior is of great interest around the world (Huyen *et al.* 2017; Nasseri *et al.* 2017; Ojeda-Bustamante *et al.* 2017). On the other hand,

doi: 10.2166/wcc.2020.142

urbanization is an important man-made factor that may disturb the watershed water cycle (Altdorff *et al.* 2017; Thakur *et al.* 2017). The influence on the underlying surface in an urbanizing watershed is acute. The increasing proportion of land-use areas with impermeable cover for new settlements will alter the original runoff and infiltration mechanisms that are critical for watershed hydrological processes. There is a great demand for quantitative descriptions of the hydrological process and its responses to both climate change and land-use conversion in an urbanizing watershed (Chawla & Mujumdar 2015; Nadal-Romero *et al.* 2016; Talib & Randhir 2017).

Scenario analysis is a valid approach to analyze possible responses of the watershed hydrological process to alternative possible regional conditions in the future (Bellin *et al.* 2016; Joorabian Shooshtari *et al.* 2017). Different integrated model applications have been designed and used to represent various possible climate changes and land-use conversions in the future and to estimate potential impacts from these individual and/or combined changes on watershed hydrological processes in quantity, stability, and uncertainty (Lin *et al.* 2007; Shi *et al.* 2013; Tan *et al.* 2015; Fernandes *et al.* 2016; Rouholahnejad Freund *et al.* 2017; Joseph *et al.* 2018). Previous studies have found various responses for regional water resources in the changes of climate and land use in different areas. The increase in precipitation would lead to more potential streamflow, but the higher temperature would lead to less streamflow resulting from the increase of evapotranspiration. The more impervious surface from urbanized land-use cover would lead to more water transfers from a runoff route that forms streamflow more easily but is consumed by evapotranspiration. In addition, the combined effects of climate and land-use change on hydrological processes were intricate and of great concern in recent studies (Marhaento *et al.* 2018; Wang & Kalin 2018). Generally, the response of the hydrological process would be different in different areas, and it is important to obtain estimations for various watersheds. The main objective of the study is to address the changes of watershed hydrological variables under various individual and combined scenarios of climate change and urbanization with proper model approaches in a watershed in northwest China.

As a source tributary of the Yellow River, the Jing River was used as a study case in this paper. Given that it is critical for regional water resource management, it is important to estimate its hydrological response to future changed environments with proper model applications. However, the available data for the study area were limited, and establishing a valid modeling scheme is of great significance. In this study, we proposed an integrated multimodel approach to estimate the responses of hydrological processes to modeled future climate change and land-use conversion scenarios for the Jing River watershed. The hydrological model of Generalized Watershed Loading Function (GWLF) was employed as the modeling tool for the watershed hydrological estimation here, because its modest data requirement was able to be satisfied with the existing data from the study watershed. The Land Change Modeler (LCM) for ArcGIS was operated with its multilayer perceptron neural network function for future land-use predictions. Considering the spatial accuracy of the GWLF model, future climate changes were estimated in overall watershed scale. As a cultivated and woodland-dominated watershed with a small proportion of the urban area, there would be an assumption of stationarity for watershed climate status, and the weather generator model of the Long Ashton Research Station Weather Generator (LARS-WG) was eligible for the statistical downscaling analysis (Salvi *et al.* 2016). In addition, the spatial non-uniform and local instability caused by urban heat island effect from an increased urban area were ignored (Shastri *et al.* 2019), and various synthetic sequences of daily weather variables generated by the LARS-WG based on different GCM outputs were used in GWLF for the hydrological response assessment. All three models have been widely applied in their own domains, and benefit from their coherences in scope, the potential of multimodel linkages is concerned and tested for a reliable assessment, to the status of future watershed hydrological processes considering the synergistic effects of climate change and urbanization.

METHODS

Study area and data source

This study was conducted in the Jing River watershed, located in northwestern China. The Jing River extends from the eastern side of Liupan Mountain and drains into

the Wei River, which is the largest tributary of the Yellow River. The portion of the Jing River watershed located above the Jing-Chuan Hydrologic Gauge Station was used as the study area. The area of the study watershed is approximately 3,145 km^2, with a mean daily temperature of 9.03 °C and a mean annual precipitation of 503.31 mm. It is a multiple land-use watershed with upland forest and grass in upstream areas and considerable cultivated land in downstream areas along the river. Ping-Liang City is located in the study watershed. It is surrounded by a number of small villages and experiences critical pressure from water resource shortages. The area of Ping-Liang City increased by over 150%, with significant population growth in the past few decades, indicating a significant demand for response estimations and predictions of future water resources to support local management. The main geographical and environmental attributes of the study watershed are shown in Figure 1, and the sources of the original data used in this study are summarized in Table 1.

Application of GWLF

The GWLF model was employed to model watershed hydrological processes (Haith & Shoemaker 1987). It was used

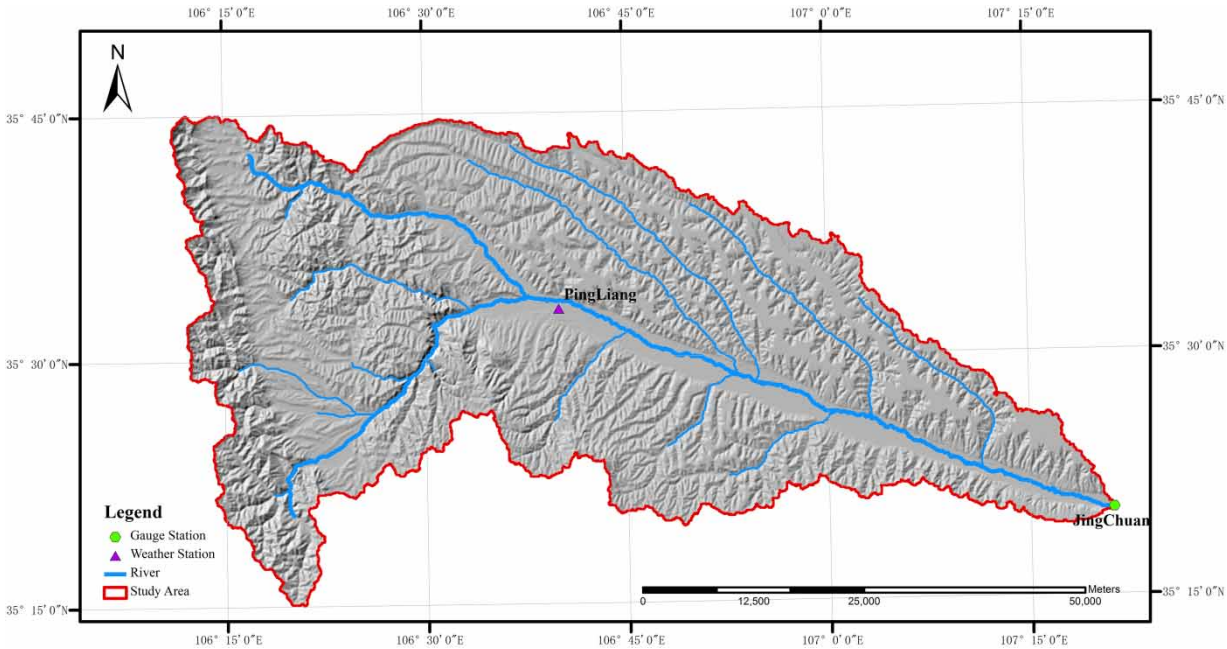

Figure 1 | Geographic location and watershed spatial attributes of the study area.

Table 1 | Summary of the original input data source used in this subject

Name	Source	Resolution	Remark
Digital elevation model	Geospatial Data Cloud site, Computer Network Information Center, Chinese Academy of Sciences (http://www.gscloud.cn)	30 m * 30 m raster	ASTER GDEM V2
Land-use cover maps	The dataset is provided by Data Center for Resources and Environmental Sciences, Chinese Academy of Sciences (RESDC) (http://www.resdc.cn)	30 m * 30 m raster	Periods of 2000, 2010 and 2015
Weather data	Climatic Data Center, National Meteorological Information Center, China Meteorological Administration (http://data.cma.cn)	Daily	From 1955 to 2014
Hydrological records	National Earth System Science Data Sharing Infrastructure, National Science & Technology Infrastructure of China (http://www.geodata.cn) and 'Annual Hydrological Report PR China'	Monthly streamflow	1956–1963, 1971–1990, and 2006–2014

here due to its moderate data requirement, which can be satisfied based on a basic public dataset in China for the study area. The GWLF is considered to be a combined distributed and lumped parameter watershed model with broad applications (Jennings *et al.* 2009; Hong *et al.* 2012; Qi *et al.* 2019). For surface runoff estimations, the GWLF is distributed in the sense that it divides multiple homogenous land-use areas based on the Soil Conservation Service Curve Number (SCS-CN) method. For subsurface groundflow estimations, the model acts as a lumped parameter model with a linear groundwater reservoir to describe the shallow saturated subsurface zone and calculate flow yields. A daily water balance approach is operated to hold the daily hydrological process estimation, and reliable monthly model results can be achieved by ignoring the spatial routing of streamflow, with the assumption that the travel times are significantly less than 1 month. A new segment function approach for the saturated zone and leakage transport approach for the unsaturated zone based on a previous study were added to obtain better estimations during low-flow periods (Sha *et al.* 2014a).

The Regional Nutrient Management (ReNuMa) software that uses the same hydrological model components as the GWLF was used in this study due to its flexible operation and powerful embedded calibration procedure – the Generalized Likelihood Uncertainty Estimation (GLUE), which was adopted for model calibration and uncertainty estimations for the study area (Sha *et al.* 2013, 2014b; Hu *et al.* 2018). The observed monthly streamflow records from 1971 to 1990 were used in the calibration process, while the records of 1956–1963 and 2006–2014 were reserved for verification. The sensitive transport parameters determined by an advanced sensitivity analysis were calibrated by a GLUE Bayesian analysis. The prior distributions for each parameter were set as the default ranges from the GWLF manual, and 100,000 groups of parameter sets were sampled followed by the same number of model iterations to build a reliable likelihood function distribution based on the contrast of modeled and observed data for the calibration period. The Nash–Sutcliff coefficient (R^2_{NS}) was used to measure model accuracy, and a value of 0.80 for R^2_{NS} was set as the cutoff threshold for posterior sampling to determine the parameters' distributions as well as the uncertainty of the results. The calibrated GWLF could then be used to estimate the responses of hydrological processes to various changes in environmental factors.

Application of the LCM

The LCM is a software extension for ArcGIS developed by Clark Labs (Eastman *et al.* 2005). Being a powerful tool, the LCM has been widely used for the assessment and prediction of land cover change and its implications (Fuller *et al.* 2011; Sangermano *et al.* 2012). The LCM first analyzes the historical change between two land cover maps of different time periods defined by the user. For each significant change from one land-use type to the other, several dynamic or static environmental variable maps that potentially drive or explain such change are incorporated to create a transition potential map that expresses the likelihood of land cover conversion in the future by using one of three alternative methodologies: Logistic Regression, a MultiLayer Perceptron (MLP) neural network, and the similarity Weighted Instance-based Learning algorithm. With the group of potential maps and the transition probability matrix from an automatic internal Markov Chain analysis or a user-defined external model file, the prediction map of future land cover can be output based on a multiobjective land competition model with a single realization, together with an optional "soft" prediction output that provides a comprehensive assessment of the change potential for a habitat and biodiversity assessment.

In this study, there were 13 land-use types that existed in the study area, and the land-use maps in 2000 and 2010 were used as the earlier and later land cover images, respectively. The change analysis was operated by the LCM, and five significant transitions that were greater than 1 km^2 were of concern, including cultivated land to shrubbery lands, middle coverage grassland, cities and towns, and rural residential land, as well as other forestland to cities and towns. Six potential driving or explanatory variable maps were employed, including elevation, slope, distance to road, distance to city, and distance to village. These maps were evaluated for each transition between two land-use types by using the MLP neural network to select the best combination and create related submodels and transition potential maps, based on which future land cover maps could be predicted. The land-use map of 2015 was used for validation, and the land-use maps of 2050 and 2080 were modeled with a Markov

Chain process to represent land cover conversion linked to the GWLF model to estimate future hydrological processes.

Application of the LARS-WG

The LARS-WG stochastic weather generator was used for the downscaling analysis to obtain a future synthetic weather time series (Semenov & Barrow 1997). It uses a series of semi-empirical distributions to describe weather factors, the parameters of which are calibrated and validated with long-term observational weather data records. The LARS-WG has a significant capability to reproduce the stationarity weather condition with the implicit assumption that history would repeat itself and the statistical characteristics based on historical weather records would be still valid for the future. In addition, by updating the model parameters based on a logical hypothesis and/or model prediction, the LARS-WG can generate a suite of synthetic daily weather variables that represent future climate conditions (Chen *et al.* 2013; Hassan *et al.* 2014).

In this study, 60 years of observed daily weather data from 1955 to 2014 from the Kong-Tong weather station were used for model calibration to determine the model parameters, based on which 60 years of synthetic daily weather data were generated for model validation, together with the random seed number of 541 defined in the LARS-WG model. The two groups of daily weather data were compared to test the model validity. The Kolmogorov–Smirnov (K–S) test was used to assess the consistency of seasonal wet/dry series distributions, daily precipitation distributions, daily minimum temperature distributions, and daily maximum temperature distributions. The *t*-test was used to judge the consistency of the monthly mean of precipitation, the monthly mean of the daily minimum temperature, and the monthly mean of the daily maximum temperature. The consistency of the monthly variances of precipitation was tested by the *F*-test.

The three main projected emission scenarios of A1B, A2, and B1, proposed by the Intergovernmental Panel on Climate Change (IPCC)'s Special Report on Emissions Scenarios (SRES) storylines in the Fourth Assessment Report (AR4), were considered with regard to two future periods of 2046–2065 (2050s) and 2080–2099 (2080s). The A1B scenario described a future world of very rapid economic growth, where the global population peaks at mid-century and declines thereafter, with the rapid introduction of new and more efficient technologies that are balanced across energy sources. The A2 scenario describes a very heterogeneous world of self-reliance and preservation of local identities with a continuously increasing population, regionally oriented fragmented economic development, and a slow technological change. The B1 scenario describes a convergent world with the same global population as A1B but with rapid changes in economic structures moving toward a service and information economy based on clean and resource-efficient technologies. New scenarios of Representative Concentration Pathways based on radiative forcing levels had been released in IPCC AR5, but we still employed the socio-economic SRES scenarios of A1B, A2, and B1 in AR4 for this study area; SRES scenarios integrated the influence of population, land use, and technology on climate on a large regional and/or global scale, and the influence of changed climate status on the local hydrological process could be further magnified for small watersheds with acute land cover conversions. The AR4 scenarios had the capability to represent the climate change influences on the hydrological process from multiple human activities and were widely applied for a response estimation in urbanizing areas (Benini *et al.* 2016; Rouhani & Jafarzadeh 2018; Wang & Kalin 2018).

To quantify the changes of climatic factors under various AR4 scenarios, six general circulation models (GCMs) were employed, including HADCM3, GFCM21, INCM3, IPCM4, MPEH5, and NCCCSM. The outputs of each GCM had already been embedded into the LARS-WG in advance. An ensemble approach is adopted by using mean values of multi-GCMs to avoid uncertainty from using one single GCM, based on which the calibrated LARS-WG parameters were updated to generate future synthetic weather data series. Sixty years of synthetic daily weather data were generated for each scenario in one future period to represent the predicted climate conditions in the study area, which could be further used as input weather data for the GWLF to estimate the hydrological response.

A flow chart was provided in Figure 2 to illustrate the process of this study.

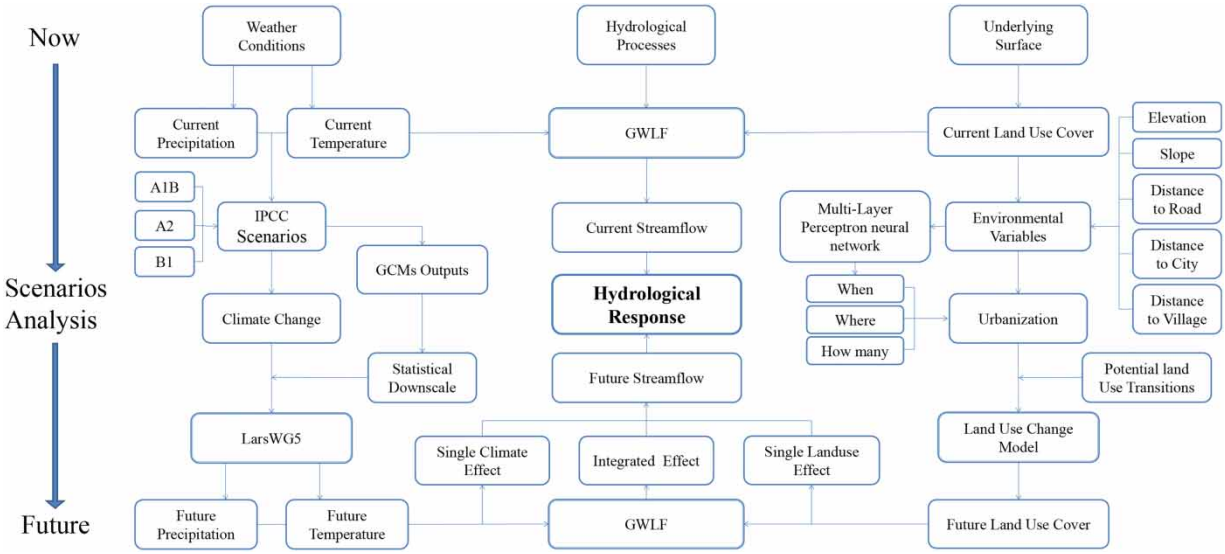

Figure 2 | The flow chart of the study.

RESULTS AND DISCUSSION

Model outputs

Hydrological model

The time series of the observed and modeled monthly streamflow during the research period are illustrated in Figure 3. In the calibration period, both the R^2_{NS} and the coefficient of determination were 0.83. In the validation period, the value of R^2_{NS} was 0.76, and the coefficient of determination was 0.77. The main calibrated model parameters are summarized in Table 2, and the posterior mean values were used for further response estimations. The model results showed excellent goodness of fit for outputs, indicating that the calibrated GWLF model could provide reliable model estimates of streamflow.

Land-use change model

The results of the MLP neural network in the LCM for each land-use cover transition are listed in Table 3. All accuracy rates were higher than 85%, and all the skill measures were higher than 0.75, indicating that the selected variable maps could drive and/or explain the land cover changes,

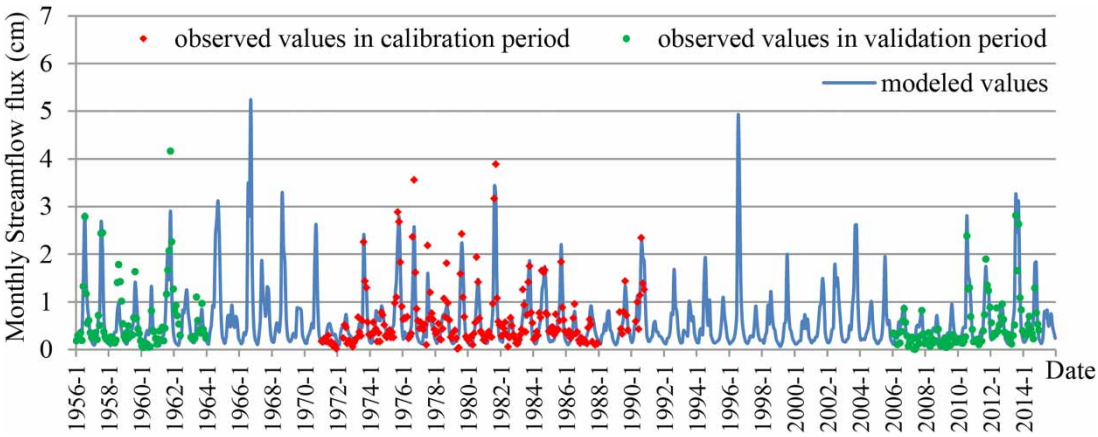

Figure 3 | Time series of observed and modeled monthly streamflow during the research period.

Table 2 | Calibrated results of GWLF hydrological transport parameters

Parameter items	Subcategories	Bayesian posterior distributions	
		Mean	Standard deviation
Runoff curve number	Cultivated land	48.69	8.74
	Wood land	24.20	4.65
	Shrubbery lands	28.26	5.61
	Sparsely forested woodland	27.82	5.24
	Other forest land including garden	36.78	6.99
	High coverage grassland	47.54	9.12
	Middle coverage grassland	54.91	9.90
	Low coverage grassland	66.05	12.75
	Reservoir and pond	100.00	1.84
	Bottomland	99.16	1.82
	Cities and towns	99.23	1.10
	Rural residential land	91.49	13.91
	Other developed land	99.79	19.78
Evapotranspiration cover factor	Jan	0.51	0.09
	Feb	0.50	0.10
	Mar	0.49	0.09
	Apr	0.62	0.11
	May	0.59	0.11
	June	0.54	0.09
	July	0.52	0.08
	Aug	0.58	0.10
	Sep	0.63	0.11
	Oct	0.50	0.10
	Nov	0.50	0.10
	Dec	0.50	0.10
Groundwater flow	Recession coefficient	0.0122	0.0019
	Seepage coefficient	0.0305	0.0049
	Slow recession coefficient	0.0130	0.0022
	Slow seepage coefficient	0.0004	0.0001
	Groundwater limit for recession	0.6730	0.1284
	Groundwater limit for seepage	0.7053	0.1208
	Unsaturated zone leakage coefficient	0.2503	0.0329

Table 3 | Results of the MLP neural network in the land change modeler

Land-use transitions	Variables*	Hidden layer neurons	Accuracy rate (%)	Skill measure
Cultivated land to cities and towns	1, 4, 6	2	98.65	0.9730
Cultivated land to rural residential land	2, 3, 4	3	90.89	0.8178
Cultivated land to shrubbery lands	2, 3, 6	4	91.32	0.8263
Cultivated land to middle coverage grassland	1, 2, 3, 4, 5, 6	5	86.26	0.7251
Other forest land including garden to cities and towns	2, 4, 6	2	88.03	0.7606

*This item indicated the variables selected and used for driving or explaining the land-use transition, which were numbered for short in the table:
1: Digital elevation model map.
2: Slope map.
3: Distance to rural residential land, which is dynamic to be updated during calculation.
4: Distance to cities and towns, which is dynamic to be updated during calculation.
5: Distance to river, which is dynamic to be updated during calculation.
6: Distance to road.

and the transition potential maps were qualified for future land-use cover predictions.

Concerning the model validation results, all the relative errors between the modeled and real changes from 2010 to 2015 for each land-use type were lower than 20%, and with such transition features in the 2000s, there would be significant increases of cities and towns as well as rural residential land in 2050 and 2080 (Table 4). In

Table 4 | Results of the land change modeler

Land-use type	Relative error in validation (%)*	Area in 2010 (km^2)	Area in 2050 (km^2)	Area in 2080 (km^2)
Cultivated land	1.83	1,233.01	982.42	793.84
Shrubbery lands	3.76	163.89	181.14	193.19
Other forest land including garden	15.98	11.10	6.31	4.55
Middle coverage grassland	1.25	942.36	1,077.97	1,172.18
Cities and towns	6.53	15.20	73.84	128.35
Rural residential land	1.62	107.28	151.16	180.74

*The relative error indicated the changes of area for each land-use type from 2010 to 2015 between modeled and real maps.

comparison to the baseline level of 2010, the area of cities and towns would increase by 3.9 times in 2050, and almost 73% was converted from cultivated land. The area of cities and towns would increase by 7.4 times in 2080, more than 83% from cultivated land. The rates of increase in rural residential land were 41 and 68%, respectively, in 2050 and 2050, which were also mainly changed from cultivated land. The area of cultivated land would keep decreasing, while the scrubland and grassland would increase in accordance with the "returning farmland to forest or grassland" policy of the Chinese government. The results of the LCM showed that the whole studied watershed had an obvious urbanizing trend in the future (Figure 4). Other detailed model results can be found in the Supplementary Material.

Climate change model

The simulated and observed mean monthly precipitation and standard deviation, as well as the monthly mean of the daily maximum and minimum temperature, are shown in Figure 5. The results showed that the errors in precipitation simulations mainly occurred in the summer months with high precipitation, and the simulations of temperature matched well in all months. In another view, the results of the statistical tests between the observed and modeled daily weather data showed that there were only small ratios of significantly different results at the 5% significance level out of the total number of tests. Only monthly variances of precipitation and the monthly mean of the daily minimum temperature had several significantly different

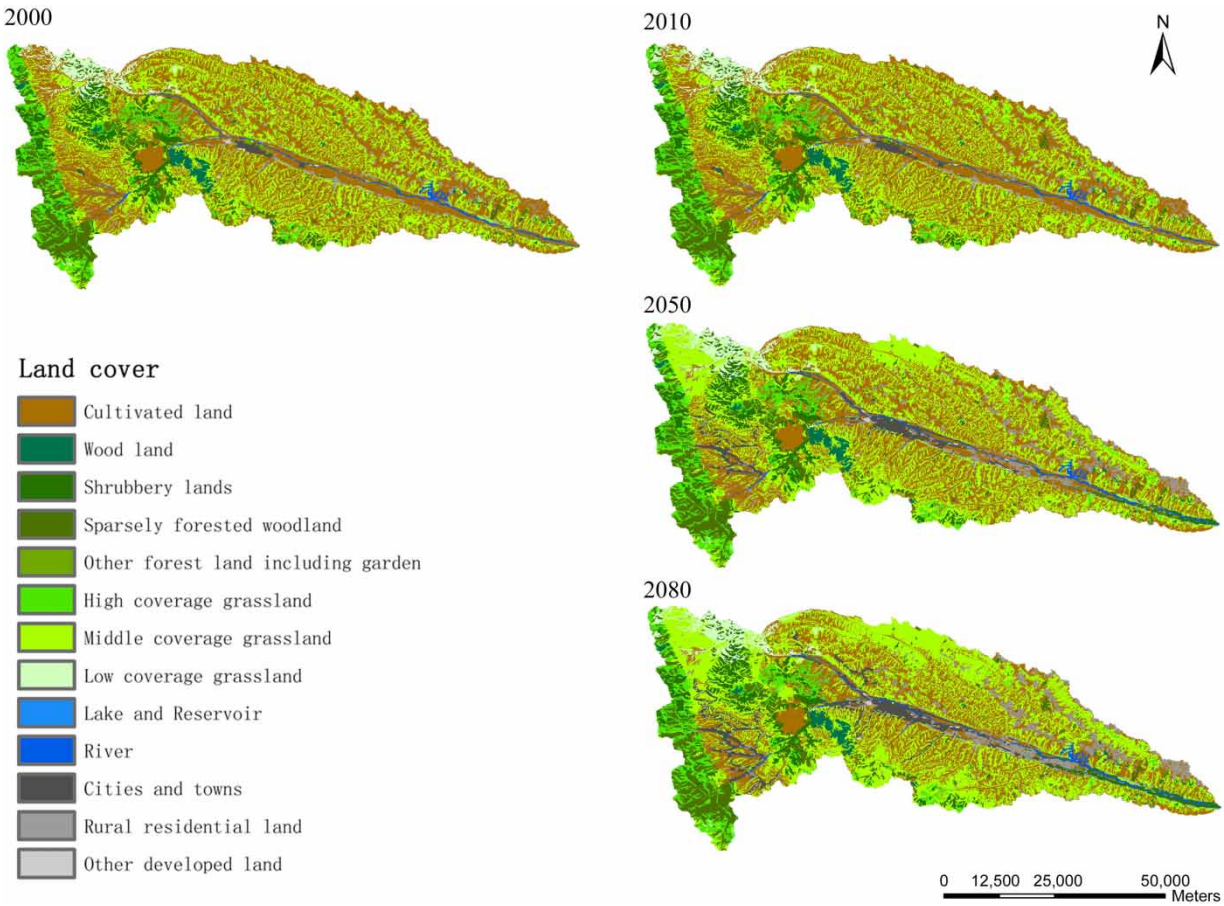

Figure 4 | Contrasts of the spatial distribution of land cover in 2000, 2010, 2050, and 2080.

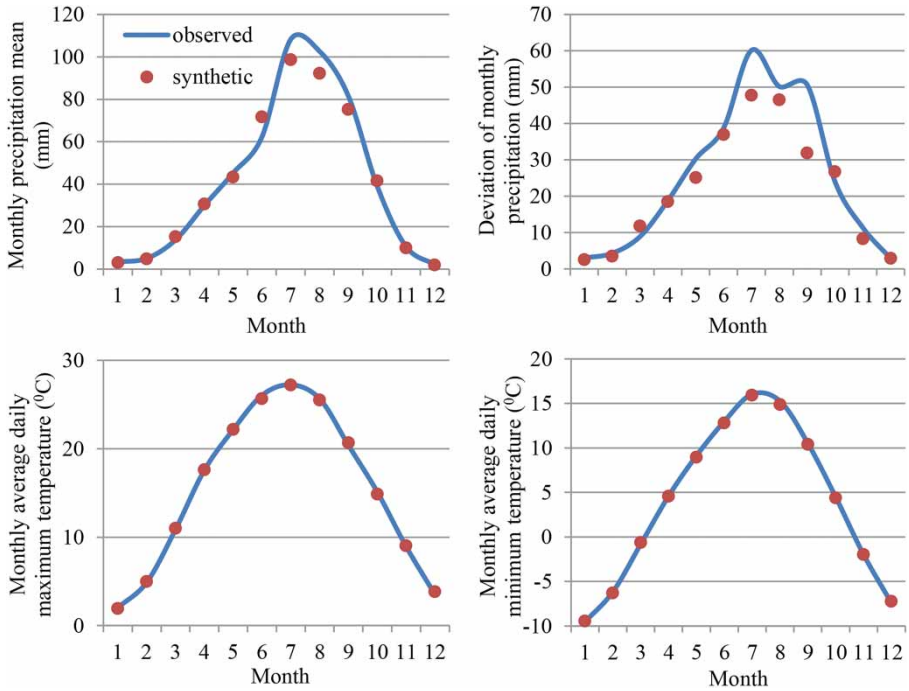

Figure 5 | Comparisons of the observed precipitation and temperatures to the simulated values from LARS-WG.

results with low percentages, in accordance with the graphic comparisons. The model performance can be classified as excellent compared with other similar model applications (Abubakari *et al.* 2018; Khorshidi *et al.* 2019), indicating that the assumption of stationarity for watershed weather is true and the calibrated and validated LARS-WG model has credible ability to generate synthetic future weather data under various climate scenarios.

The impacts of an increased urban area on watershed climate changes were ignored in this study. Urban growth can result in local instability with more extreme weather status due to the urban heat island effect and lead to non-uniform climate changes in the watershed. However, the urban area accounts for only a small part of the watershed area, just 0.6% for current and 5.2% for the most extreme urbanization scenario based on the LCM model results (Table 4). In addition, the nonstationary changes in the urban region may also affect the surrounding watershed area, and these nonuniformities in space could be ignored when we focus on the overall watershed level for hydrological response estimations. Thus, only global climate change scenarios were used to estimate watershed temperature and precipitation changes considering various storylines for human society including large-scale land-use changes, which is suitable to estimate watershed climate changes for GWLF application. The mean values of six GCM outputs that represented the future change intensity of the main climatic factors on a monthly scale were calculated and used to update the parameter set of the LARS-WG model (Table 5). For each scenario and future period, 60 years of synthetic daily weather data were generated, which were further used as input weather data of the GWLF for the estimation of future hydrological processes, the results of which are discussed in the section "Conclusion". More detailed descriptions about the application and model parameters of the LARS-WG are provided in the Supplementary Material.

Hydrological responses

Hydrological process in future climate changes

The changes in watershed hydrological processes under future climate conditions were estimated. Seven synthetic series of 60 years of daily weather data that indicated the current and future status were input into the GWLF, while the land-use cover from 2010 was constantly used for all

Table 5 | Changes of climatic factors in different future periods under different socio-economic scenarios based on the ensemble of six GCMs' outputs

Periods	Items / Scenarios	Relative changes in monthly mean rainfall			Absolute changes in monthly mean minimum temperature			Absolute changes in monthly mean maximum temperature		
		A1B	A2	B1	A1B	A2	B1	A1B	A2	B1
2050s	Jan	1.19	1.18	1.93	2.75	2.57	1.70	2.56	2.40	0.97
	Feb	1.18	1.18	1.73	2.69	2.46	1.51	2.43	2.26	0.98
	Mar	1.15	1.17	1.70	2.58	2.36	1.49	2.28	2.10	0.98
	Apr	1.13	1.13	1.72	2.60	2.36	1.50	2.30	2.10	0.98
	May	1.09	1.05	1.64	2.62	2.34	1.52	2.46	2.23	1.00
	June	1.04	0.98	1.72	2.63	2.31	1.74	2.61	2.36	1.03
	July	1.00	0.95	1.89	2.63	2.35	2.03	2.74	2.51	1.05
	Aug	1.00	0.98	1.86	2.55	2.34	2.10	2.80	2.56	1.03
	Sep	1.07	1.08	1.77	2.46	2.24	1.97	2.70	2.36	0.99
	Oct	1.09	1.09	1.84	2.49	2.28	1.88	2.56	2.24	0.97
	Nov	1.10	1.10	1.89	2.61	2.46	1.80	2.56	2.35	0.97
	Dec	1.17	1.15	1.94	2.69	2.59	1.79	2.59	2.45	0.97
2080s	Jan	1.31	1.30	2.71	4.09	4.72	2.64	3.94	4.36	0.97
	Feb	1.30	1.24	2.70	3.90	4.70	2.57	3.66	4.30	0.98
	Mar	1.25	1.23	2.70	3.73	4.55	2.48	3.39	4.16	0.99
	Apr	1.19	1.19	2.58	3.74	4.43	2.31	3.43	4.10	1.00
	May	1.13	1.13	2.39	3.64	4.30	2.25	3.53	4.16	1.00
	June	1.07	1.09	2.36	3.59	4.20	2.40	3.69	4.29	1.02
	July	1.01	1.04	2.56	3.65	4.33	2.69	3.85	4.56	1.04
	Aug	1.04	1.02	2.66	3.68	4.47	2.87	3.93	4.75	1.04
	Sep	1.11	1.09	2.52	3.69	4.30	2.74	3.90	4.54	1.01
	Oct	1.10	1.15	2.44	3.69	4.15	2.56	3.74	4.29	0.99
	Nov	1.13	1.24	2.52	3.76	4.29	2.52	3.68	4.29	0.98
	Dec	1.24	1.34	2.64	3.95	4.55	2.60	3.85	4.35	0.97

scenarios as the base level. The main model outputs concerning the hydrological factors of streamflow, runoff, groundwater flow, and evapotranspiration, together with precipitation and air temperature, are compared in Figure 6.

The results showed that there will be a general increasing trend for annual streamflow in the future. For the A2 scenarios, a continual slight increase occurred, and for the A1B scenario, there would be a rapid increase in the 2050s but a significant decrease in the 2080s that approach the baseline level. The change for the B1 scenario was generally steady in the 2050s and significantly increased in the 2080s, with the expected mean value of annual streamflow approximately 10.7% higher than the baseline level. The change in the behavior of groundwater flow was similar to that of streamflow, but the behavior of the runoff represented a continual increase for all three climate scenarios. Because of the increase in air temperature in the future, evapotranspiration also showed a large increase, the intensities of which corresponded to the changes in temperature for different climate scenarios in different periods. There would also be more precipitation in the future that could offset the additional loss of water from evapotranspiration and finally result in an increasing water flux for the study watershed.

In addition, the streamflow values in extreme high flow years were concerned with the mean values of the top 5% highest annual streamflow for each scenario and the baseline level. The change in the behavior of high annual

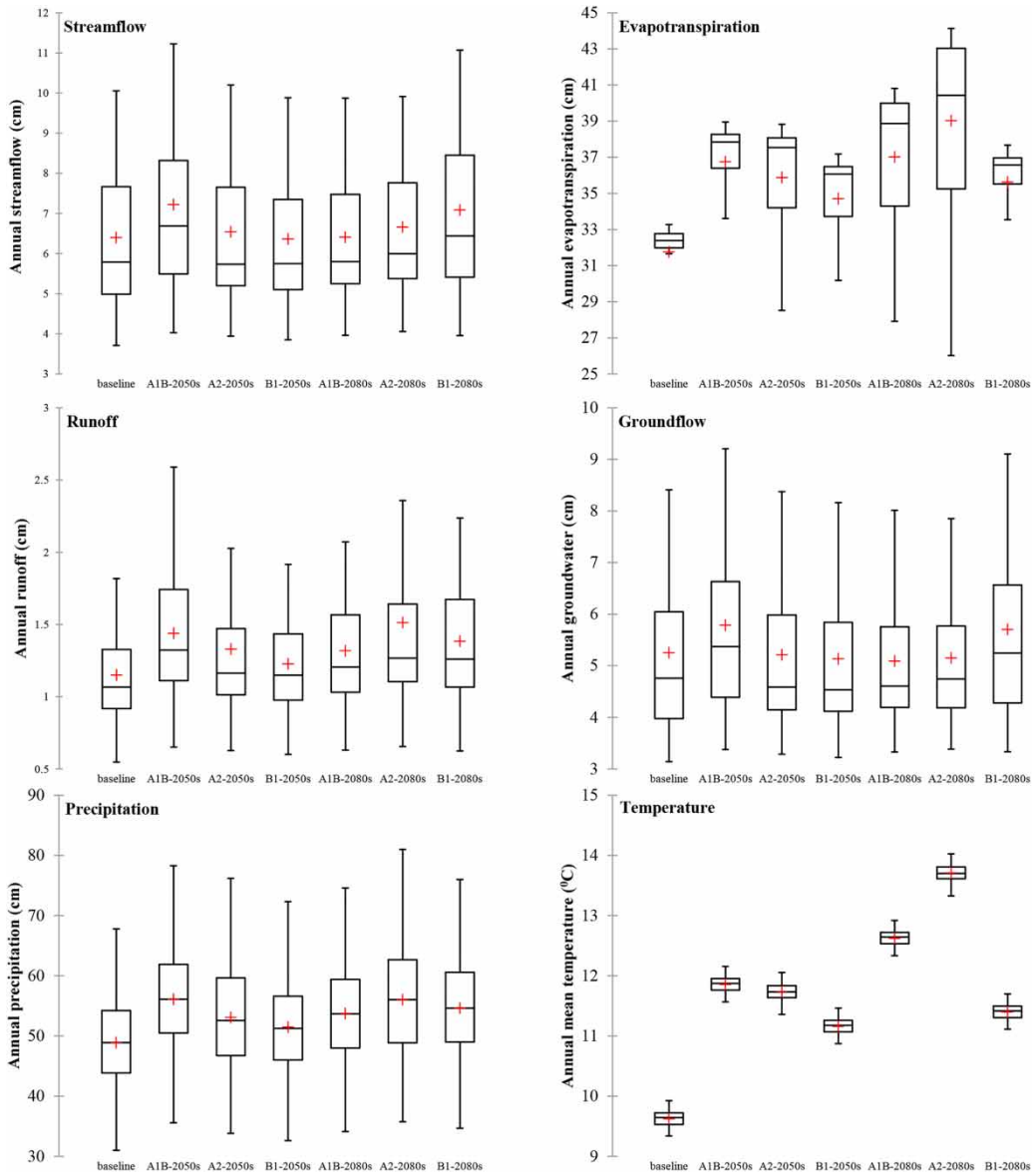

Figure 6 | The responses of hydrological processes to future climate changes on an annual scale. The upper and lower borders of the box represent the 25th and 75th percentiles, respectively; the line and cross in the box interior represented the median and mean values, and the "whiskers" were the minimum and maximum values.

streamflow was similar to that of the mean value but had a greater increase in intensity. The mean rate of increase of the extreme annual streamflow for B1 scenarios in the 2080s would be 12.1%, higher than the 10.7% from mean value-based statistics. In addition, the increase of extreme annual streamflow for A1B scenarios in the 2050s would be more than 15%. These results implied a greater flood risk under future climate conditions, which should be of great concern for local water resource management. The increasing trends of streamflow were different with other cases (Benini et al. 2016; Farjad *et al.* 2016; Rouholahnejad Freund *et al.* 2017), particularly for the significant increase in A1B scenarios in the 2050s, implying a significant interaction between global economic and population growth and urbanizing watershed streamflow.

In addition, the changes in climate conditions would also convert the initial monthly apportionment of critical hydrological factors (Figure 7). As a result of the rise in air

Figure 7 | The changes in the monthly hydrological factors in future climate conditions.

temperature, the evapotranspiration increased in all months, among which the winter months had a higher rate of increase, but most evapotranspiration still occurred in the hot months, consistent with the temperature. Most months in the future will have more precipitation. The future monthly runoff would generally increase, except in February and October, and the monthly groundwater flow would increase in the winter but probably decrease in the summer and autumn, particularly for the A2 scenario. The streamflow was commonly determined by precipitation, evapotranspiration, runoff, and groundwater flow processes, and the increases in future streamflow would be mainly focused in the spring and summer months, with several decreases in the autumn months for the A2 scenario. The change of monthly streamflow in the study area was different from that of another urbanizing watershed, where there were greater streamflow values in the fall and winter months but no clear change in the summer (Wang & Kalin 2018). This implied that the increase of precipitation in the study area in the summer would be considerable and could counteract the decrease of evapotranspiration from future hotter weather. In addition, the higher

temperature would significantly impact the forms of precipitation in the winter and shorten the freeze period, which could disturb the original snow storage and thaw behaviors and lead to obvious changes in hydrological processes, particularly for higher intensity evapotranspiration in the winter in future climate conditions.

Hydrological process in future land-use conversions

The changes of watershed hydrological processes under future land-use cover conditions were estimated. Predicted areas for each land-use type in the 2050s and 2080s were imported into the GWLF to model future hydrological processes. The observed land-use cover of 2010 and 60 years of synthetic daily weather data indicating the current climate status were used to represent the base level. Four main hydrological factors, including streamflow, runoff, groundwater flow, and evapotranspiration, were compared on both annual and monthly scales, the results of which are shown in Figure 8.

The results showed that for future changed land-use situations, there will be an increasing trend for streamflow and runoff but a decreasing trend for groundwater flow, which is generally consistent with other study results in the urbanizing watershed (Sunde *et al.* 2018; Suttles *et al.* 2018; Wang & Kalin 2018). The mean annual streamflow will increase by 12.7 and 24.3% in the 2050 and 2080s, respectively, and the increased streamflow was mainly focused in the hot months. The changes in the monthly streamflow in the winter would be slight and even show continual decreasing trends in November and December. Most new urbanized land-use cover was transformed from cultivated land, which would lead to a more impervious surface in the study area. The positive impacts from predicted land-use conversions to watershed runoff were significant. All the monthly runoff amounts would increase in the future, and the mean annual runoff would increase by 91.4 and 137.9% in the 2050 and 2080s, respectively, compared with the current level. For more insight into the source apportionment, a significant proportion of runoff came from urban land-use areas, such as cities and towns, rural residential land, and other developed land, which had obvious increasing trends for an urbanizing watershed. With impermeable surfaces, most precipitation becomes runoff transported through the municipal drain network and/or surface flow into the river. The percentage of runoff from the urban land-use area was 46.3% in the baseline period and then increased to 71.9 and 80.4% in the 2050 and 2080s, respectively, indicating a significant increasing trend of runoff with watershed urbanization. However, the response of the yield in the watershed groundwater flow to urbanized land-use conversion was negative. All monthly groundwater flows will decrease in the future with greater intensity in the autumn, and the mean annual groundwater flow will decrease by 4.5 and 8.4% in the 2050 and 2080s, respectively. These situations might result from the decrease of infiltration due to the increasing runoff with more impermeable surfaces in the future urbanized watershed. The changes in evapotranspiration with future land-use were slight, with several decreases in hot months due to the reduction of potential evapotranspiration, since the water had been transported through runoff with a quicker pathway on impermeable surfaces. To sum up, the changes of land-use cover in an urbanizing watershed would significantly disturb the original hydrological processes through more impermeable surfaces that caused the increase in runoff as well as streamflow, indicating that initiative integrated projects were greatly needed for urban development with more water conservation capacity, such as a sponge city (Mei *et al.* 2018).

Integrated hydrological change assessments

The integrated responses of watershed hydrological processes in future climate and urbanized land-use conditions were estimated. Groups of synthetic daily weather series and predicted areas of each land-use type in the future were used as the model input for the GWLF for the scenario analyses. The changes in streamflow, runoff, groundwater flow, and evapotranspiration were estimated and discussed for the combined effects of climate change and land-use conversions on the hydrological process (Figure 9). The results showed that there would be more streamflow in the future. The annual streamflow yield would keep increasing, and the streamflow in most months had positive changes compared with the baseline values. The increases in runoff under changed future conditions were significant on both annual and monthly scales, but the changes in the annual

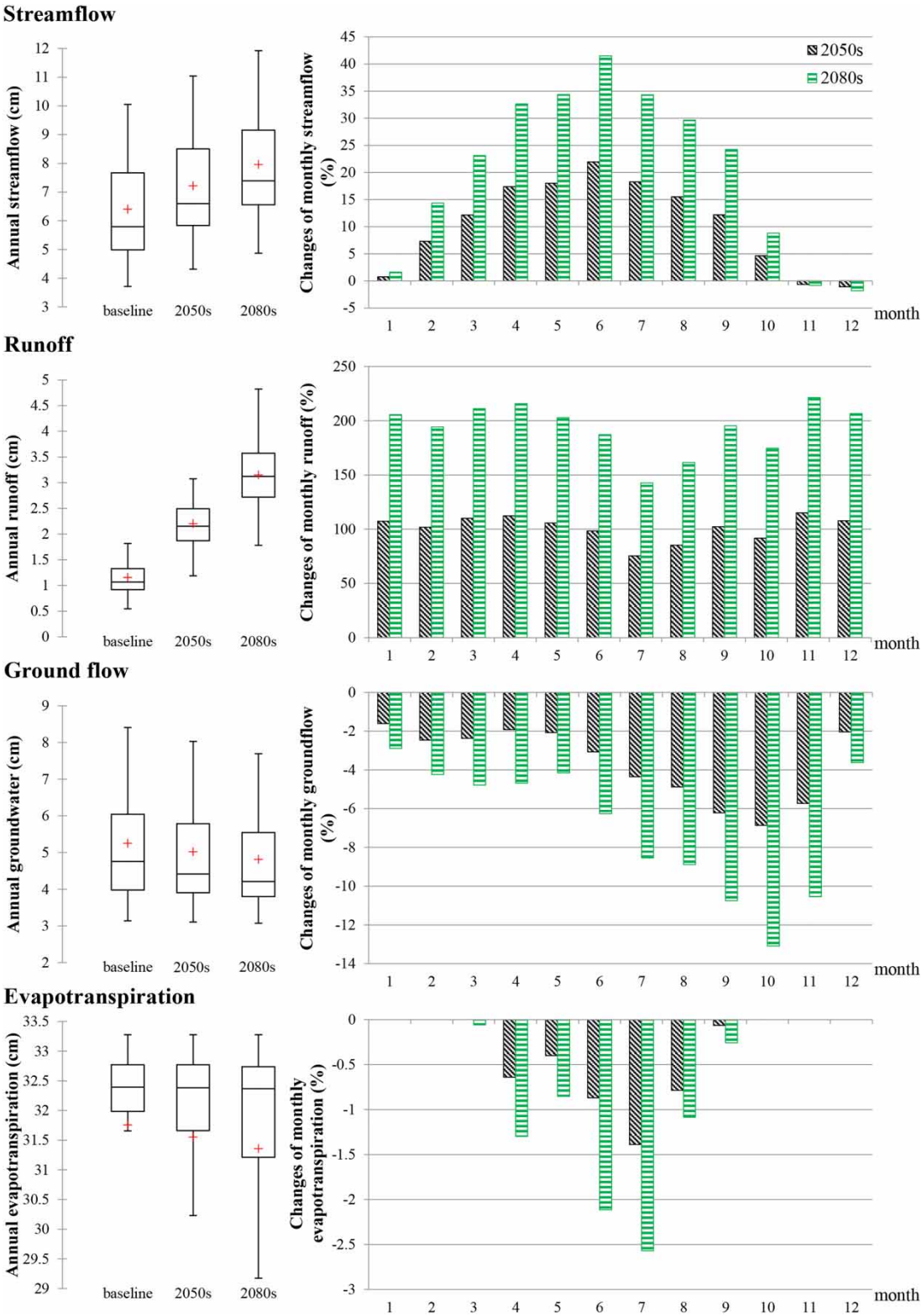

Figure 8 | The responses of main hydrological factors under future land-use cover conversions.

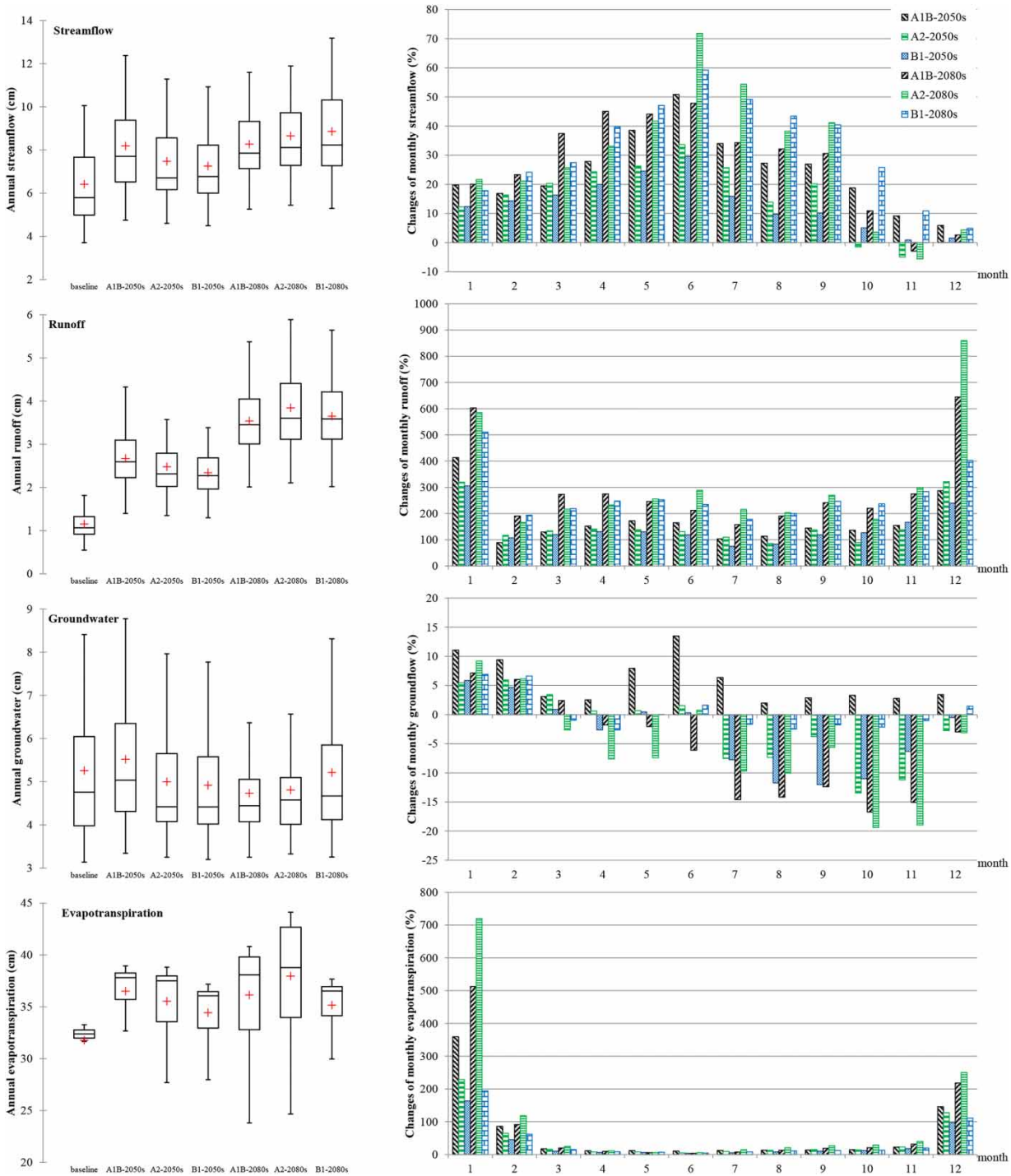

Figure 9 | The responses of the main hydrological factors under the combined effects of climate change and urbanization.

groundwater flow were opposite, in which the increase mainly existed in the spring and the decrease occurred in summer and autumn. The evapotranspiration would increase, with a high percentage in January due to the small amount of evapotranspiration in the current status. The changes of evapotranspiration were similar to the

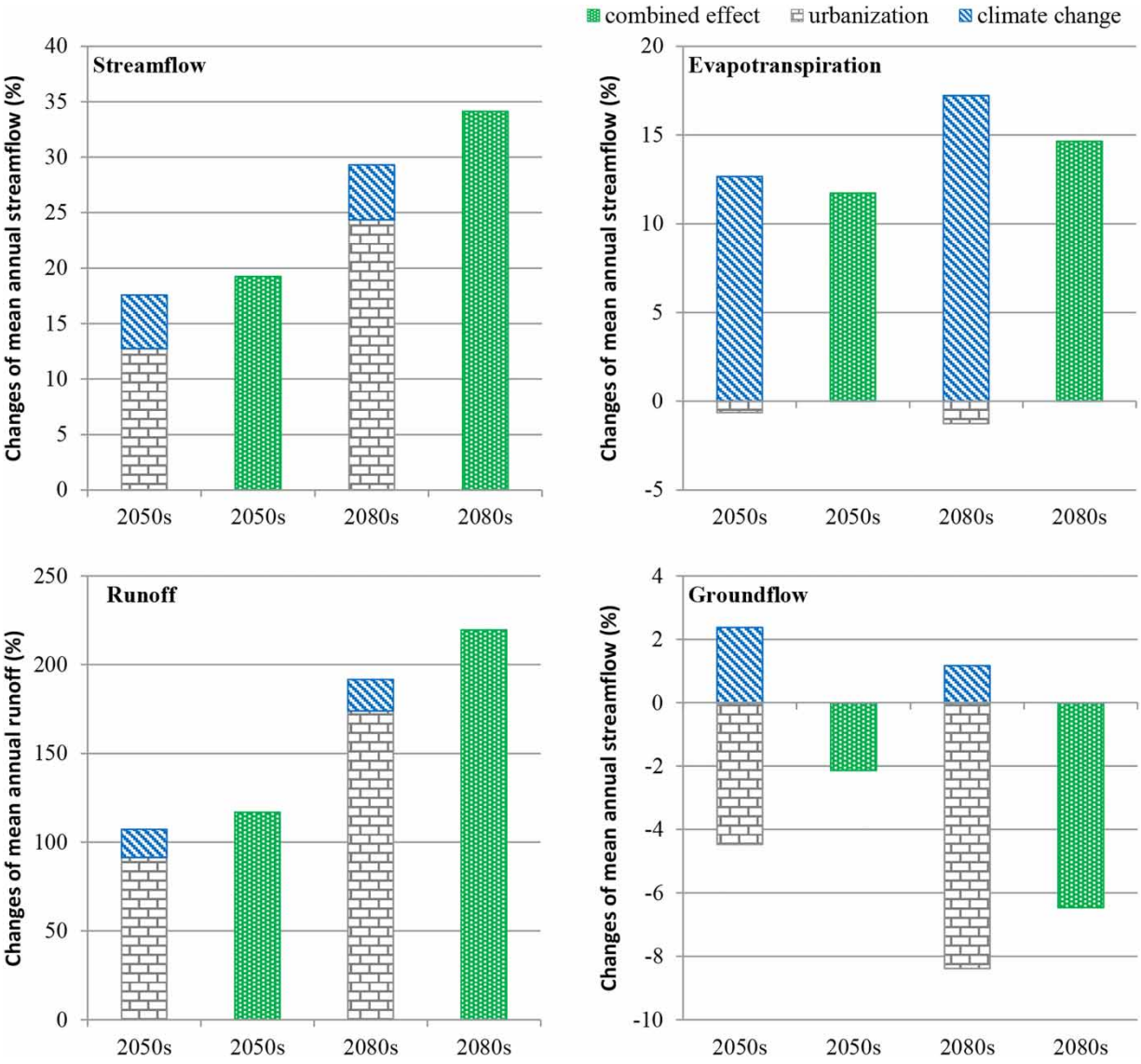

Figure 10 | Comparisons of changes in the mean annual streamflow in the two individual scenarios and the combined scenario of climate change and urbanized land-use conversions.

changes caused only by climate change due to the slight effects on the evapotranspiration from land-use conversions.

The changes in the main hydrological factors of the watershed in the combined scenario situation were further compared with the results from the two individual scenarios of climate change and urbanized land-use conversions (Figure 10). There were pronounced synergistic effects on streamflow from combined land-use and climate changes in many other studies (Molina-Navarro et al. 2014; Marhaento *et al.* 2018), and such a trend could also be found in this urbanized watershed. An ensemble approach was adopted with mean values of the three results based on the projected emission scenarios of A1B, A2, and B1 in one future period for a clearer expression. In the 2050s, the mean annual streamflow would increase by 4.8% under the ensemble climate change scenario and by 12.7% under the urbanized land-use change scenario, while the increase would be 19.2% under the combined scenario. In the 2080s, the combined scenario would lead to an increase in the streamflow of 34.1%, which would be 5.0 and 24.3%

for the two individual scenarios of climate change and urbanization, respectively. Urbanization represents a greater share of the influence on the increase in streamflow, and climate change would play a more important role in groundwater. Similarly, urbanization played a leading role in the increase of runoff, and there would be more runoff yield with the combined changes in climate and land-use cover. The urbanization would lead to decreases in groundwater, but climate change would increase the groundwater yield. The combined effect of the two individual scenarios would cause a decrease in the groundwater. For evapotranspiration estimations, the changes in climate played a dominant role that would significantly increase the annual evapotranspiration as the result of a hotter and wetter scenario in the future. The urbanization would slightly decrease the evapotranspiration yield, but this reduction would be advanced under the combined scenario together with climate change. To sum up, there was an interaction between climate change and urbanized land-use conversion that could lead to synergistic effects on the increase in streamflow from the combined scenario that was greater than the sum of the two individual scenarios. These findings would be useful for local managers as supporting information to mitigate future water resource pressure associated with land-use and climate changes in the study area.

CONCLUSIONS

This work modeled the changes of hydrological processes under projected future climate scenarios in an urbanizing watershed. Both the combined and individual effects of climate change and urbanized land-use conversions on the main hydrological factors were quantitatively estimated through an integrated multimodel linkage approach. The results showed that changes in weather and landscape conditions would significantly disturb the original water cycle of the watershed, and the proposed approach of the combined application of three models represented reliable accuracy and robust capability for hydrological response estimations.

For individual estimations of the impact of climate change, there would be more streamflow for all the projected emission scenarios of A1B, A2, and B1 in the future. With more precipitation and higher temperatures, the evapotranspiration would greatly increase, and both the groundwater flow and runoff would generally represent increasing trends. The increases in future streamflow would mainly be focused in the spring and summer months. Most monthly runoff amounts would increase, while the groundwater flow would increase in the spring months but probably decrease in the summer and autumn as the result of heavy evapotranspiration from hot weather conditions that could not be offset by the limited increase in precipitation. In addition, with a shorter freeze period from the temperature increase, there would be a smaller but earlier snowmelt, resulting in an increase in streamflow in January and February.

In another view, the individual impacts from future urbanized land-use conversions would clearly yield more streamflow, mainly focused on hot months. The runoff yield would be greatly increased as the result of more impermeable surfaces from new urban land-use areas that benefit the runoff form and transfer. The groundwater flow yield would be decreased due to less infiltration. Briefly, an urbanized watershed with more impermeable surfaces would lead to an increase of streamflow through the runoff process.

There would be a synergistic mechanism from the combined impacts of climate change and urbanization to increase the watershed streamflow yield. An additive effect exists such that the changes in the watershed streamflow from the combined effects would be greater than the sum of each individual effect. Under the integrated future scenarios, most monthly streamflows would increase. The increases in runoff were significant on both annual and monthly scales, but the increase in groundwater flow was mainly focused in the spring months, with several decreases in hot months. The changes in watershed hydrological processes would be critical for local management, such as flood risk control, water resource allocation and agriculture, and relevant sustainable policies, such as greenhouse gas emission reductions and Sponge City constructions, should be encouraged. The quantitative estimations of hydrological processes to various possible scenarios would be valuable for future watershed projects, and the multimodel linkage approach proposed in this paper could be used as a tool to realize interested scenario analysis for decision-making support in similar watersheds with modest data requirements.

ACKNOWLEDGEMENTS

This research was financially supported by the Science & Technology Development Fund of Tianjin Education Commission for Higher Education (2018KJ160). The authors acknowledge the developer of the LARS-WG and ReNuMa for the free access to the software, code, and license agreements. The dataset is provided by the Geospatial Data Cloud site, Computer Network Information Center, Chinese Academy of Sciences (http://www.gscloud.cn), Data Center for Resources and Environmental Sciences, Chinese Academy of Sciences (RESDC) (http://www.resdc.cn), Climatic Data Center, National Meteorological Information Center, China Meteorological Administration (http://data.cma.cn), and National Earth System Science Data Sharing Infrastructure, and National Science & Technology Infrastructure of China (http://www.geodata.cn). In addition, the authors would like to acknowledge Prof. Yuqiu Wang at Nankai University for his previous contributions concerning the GWLF.

SUPPLEMENTARY MATERIAL

The Supplementary Material for this paper is available online at https://dx.doi.org/10.2166/wcc.2020.142.

REFERENCES

Abubakari, S., Dong, X., Su, B., Hu, X., Liu, J., Li, Y., Peng, T., Ma, H., Wang, K. & Xu, S. 2018 Modelling streamflow response to climate change in data-scarce White Volta River basin of West Africa using a semi-distributed hydrologic model. *Journal of Water and Climate Change* **10** (4), 907–930.

Altdorff, D., Galagedara, L. & Unc, A. 2017 Impact of projected land conversion on water balance of boreal soils in western Newfoundland. *Journal of Water and Climate Change* **8** (4), 613–626.

Bellin, A., Majone, B., Cainelli, O., Alberici, D. & Villa, F. 2016 A continuous coupled hydrological and water resources management model. *Environmental Modelling & Software* **75**, 176–192.

Benini, L., Antonellini, M., Laghi, M. & Mollema, P. N. 2016 Assessment of water resources availability and groundwater salinization in future climate and land use change scenarios: a case study from a coastal drainage basin in Italy. *Water Resources Management* **30** (2), 731–745.

Chawla, I. & Mujumdar, P. P. 2015 Isolating the impacts of land use and climate change on streamflow. *Hydrology and Earth System Sciences* **19** (8), 3633–3651.

Chen, H., Guo, J., Zhang, Z. & Xu, C.-Y. 2013 Prediction of temperature and precipitation in Sudan and South Sudan by using LARS-WG in future. *Theoretical and Applied Climatology* **113** (3), 363–375.

Eastman, J., Van Fossen, M. & Solarzano, L. 2005 Transition potential modeling for land cover change. *GIS, Spatial Analysis and Modeling* **17**, 357–386.

Farjad, B., Gupta, A. & Marceau, D. J. 2016 Annual and seasonal variations of hydrological processes under climate change scenarios in two sub-catchments of a complex watershed. *Water Resources Management* **30** (8), 2851–2865.

Fernandes, M. R., Segurado, P., Jauch, E. & Ferreira, M. T. 2016 Riparian responses to extreme climate and land-use change scenarios. *Science of The Total Environment* **569–570**, 145–158.

Fuller, D. O., Hardiono, M. & Meijaard, E. 2011 Deforestation projections for carbon-rich peat swamp forests of central Kalimantan, Indonesia. *Environmental Management* **48** (3), 436–447.

Haith, D. A. & Shoemaker, L. L. 1987 Generalized watershed loading functions for stream flow nutrients. *Journal of the American Water Resources Association* **23** (3), 471–478.

Hassan, Z., Shamsudin, S. & Harun, S. 2014 Application of SDSM and LARS-WG for simulating and downscaling of rainfall and temperature. *Theoretical and Applied Climatology* **116** (1), 243–257.

Hong, B., Limburg, K. E., Hall, M. H., Mountrakis, G., Groffman, P. M., Hyde, K., Luo, L., Kelly, V. R. & Myers, S. J. 2012 An integrated monitoring/modeling framework for assessing human–nature interactions in urbanizing watersheds: Wappinger and Onondaga Creek watersheds, New York, USA. *Environmental Modelling & Software* **32**, 1–15.

Hu, M., Liu, Y., Wang, J., Dahlgren, R. A. & Chen, D. 2018 A modification of the Regional Nutrient Management model (ReNuMa) to identify long-term changes in riverine nitrogen sources. *Journal of Hydrology* **561**, 31–42.

Huyen, N. T., Tu, L. H., Tram, V. N. Q., Minh, D. N., Liem, N. D. & Loi, N. K. 2017 Assessing the impacts of climate change on water resources in the Srepok watershed, Central Highland of Vietnam. *Journal of Water and Climate Change* **8** (3), 524–534.

Jennings, E., Allott, N., Pierson, D. C., Schneiderman, E. M., Lenihan, D., Samuelsson, P. & Taylor, D. 2009 Impacts of climate change on phosphorus loading from a grassland catchment: implications for future management. *Water Research* **43** (17), 4316–4326.

Joorabian Shooshtari, S., Shayesteh, K., Gholamalifard, M., Azari, M., Serrano-Notivoli, R. & López-Moreno, J. I. 2017 Impacts of future land cover and climate change on the water balance

in Northern Iran. *Hydrological Sciences Journal* **62** (16), 2655–2673.

Joseph, J., Ghosh, S., Pathak, A. & Sahai, A. K. 2018 Hydrologic impacts of climate change: comparisons between hydrological parameter uncertainty and climate model uncertainty. *Journal of Hydrology* **566**, 1–22.

Khorshidi, M. S., Nikoo, M. R., Sadegh, M. & Nematollahi, B. 2019 A multi-objective risk-based game theoretic approach to reservoir operation policy in potential future drought condition. *Water Resources Management* **33** (6), 1999–2014.

Kristvik, E., Muthanna, T. M. & Alfredsen, K. 2018 Assessment of future water availability under climate change, considering scenarios for population growth and ageing infrastructure. *Journal of Water and Climate Change* **10** (1), 1–12.

Lin, Y.-P., Hong, N.-M., Wu, P.-J. & Lin, C.-J. 2007 Modeling and assessing land-use and hydrological processes to future land-use and climate change scenarios in watershed land-use planning. *Environmental Geology* **53** (3), 623–634.

Marhaento, H., Booij, M. J. & Hoekstra, A. Y. 2018 Hydrological response to future land-use change and climate change in a tropical catchment. *Hydrological Sciences Journal* **63** (9), 1368–1385.

Mei, C., Liu, J., Wang, H., Yang, Z., Ding, X. & Shao, W. 2018 Integrated assessments of green infrastructure for flood mitigation to support robust decision-making for sponge city construction in an urbanized watershed. *Science of The Total Environment* **639**, 1394–1407.

Milly, P. C. D., Betancourt, J., Falkenmark, M., Hirsch, R. M., Kundzewicz, Z. W., Lettenmaier, D. P. & Stouffer, R. J. 2008 Stationarity is dead: whither water management? *Science* **319** (5863), 573–574.

Molina-Navarro, E., Trolle, D., Martínez-Pérez, S., Sastre-Merlín, A. & Jeppesen, E. 2014 Hydrological and water quality impact assessment of a Mediterranean limno-reservoir under climate change and land use management scenarios. *Journal of Hydrology* **509**, 354–366.

Nadal-Romero, E., Cammeraat, E., Serrano-Muela, M. P., Lana-Renault, N. & Regüés, D. 2016 Hydrological response of an afforested catchment in a Mediterranean humid mountain area: a comparative study with a natural forest. *Hydrological Processes* **30** (15), 2717–2733.

Nasseri, M., Zahraie, B. & Forouhar, L. 2017 A comparison between direct and indirect frameworks to evaluate impacts of climate change on streamflows: case study of Karkheh River basin in Iran. *Journal of Water and Climate Change* **8** (4), 652–674.

Ojeda-Bustamante, W., Ontiveros-Capurata, R. E., Flores-Velázquez, J. & Iñiguez-Covarrubias, M. 2017 Changes in water demands under adaptation actions to climate change in an irrigation district. *Journal of Water and Climate Change* **8** (2), 191–202.

Oki, T. & Kanae, S. 2006 Global hydrological cycles and world water resources. *Science* **313** (5790), 1068–1072.

Qi, Z., Kang, G., Shen, M., Wang, Y. & Chu, C. 2019 The improvement in GWLF model simulation performance in watershed hydrology by changing the transport framework. *Water Resources Management* **33** (3), 923–937.

Rouhani, H. & Jafarzadeh, M. S. 2018 Assessing the climate change impact on hydrological response in the Gorganrood River Basin, Iran. *Journal of Water and Climate Change* **9** (3), 421–433.

Rouholahnejad Freund, E., Abbaspour, K. & Lehmann, A. 2017 Water resources of the Black Sea catchment under future climate and landuse change projections. *Water* **9** (8), 598.

Salvi, K., Ghosh, S. & Ganguly, A. R. 2016 Credibility of statistical downscaling under nonstationary climate. *Climate Dynamics* **46** (5), 1991–2023.

Sangermano, F., Toledano, J. & Eastman, J. R. 2012 Land cover change in the Bolivian Amazon and its implications for REDD+ and endemic biodiversity. *Landscape Ecology* **27** (4), 571–584.

Semenov, M. A. & Barrow, E. M. 1997 Use of a stochastic weather generator in the development of climate change scenarios. *Climatic Change* **35** (4), 397–414.

Sha, J., Liu, M., Wang, D., Swaney, D. P. & Wang, Y. 2013 Application of the ReNuMa model in the Sha He river watershed: tools for watershed environmental management. *Journal of Environmental Management* **124**, 40–50.

Sha, J., Swaney, D. P., Hong, B., Wang, J., Wang, Y. & Wang, Z.-L. 2014a Estimation of watershed hydrologic processes in arid conditions with a modified watershed model. *Journal of Hydrology* **519**, 3550–3556.

Sha, J., Li, Z., Swaney, D. P., Hong, B., Wang, W. & Wang, Y. 2014b Application of a Bayesian watershed model linking multivariate statistical analysis to support watershed-scale nitrogen management in China. *Water Resources Management* **28** (11), 3681–3695.

Shastri, H., Ghosh, S., Paul, S., Shafizadeh-Moghadam, H., Helbich, M. & Karmakar, S. 2019 Future urban rainfall projections considering the impacts of climate change and urbanization with statistical–dynamical integrated approach. *Climate Dynamics* **52** (9), 6033–6051.

Shi, P., Ma, X., Hou, Y., Li, Q., Zhang, Z., Qu, S., Chen, C., Cai, T. & Fang, X. 2013 Effects of land-use and climate change on hydrological processes in the upstream of Huai River, China. *Water Resources Management* **27** (5), 1263–1278.

Sunde, M. G., He, H. S., Hubbart, J. A. & Urban, M. A. 2018 An integrated modeling approach for estimating hydrologic responses to future urbanization and climate changes in a mixed-use midWestern watershed. *Journal of Environmental Management* **220**, 149–162.

Suttles, K. M., Singh, N. K., Vose, J. M., Martin, K. L., Emanuel, R. E., Coulston, J. W., Saia, S. M. & Crump, M. T. 2018 Assessment of hydrologic vulnerability to urbanization and climate change in a rapidly changing watershed in the Southeast U.S. *Science of The Total Environment* **645**, 806–816.

Talib, A. & Randhir, T. O. 2017 Climate change and land use impacts on hydrologic processes of watershed

systems. *Journal of Water and Climate Change* **8** (3), 363–374.

Tan, X. & Gan, T. Y. 2015 Contribution of human and climate change impacts to changes in streamflow of Canada. *Nature* **5**, 17767.

Tan, M. L., Ibrahim, A. L., Yusop, Z., Duan, Z. & Ling, L. 2015 Impacts of land-use and climate variability on hydrological components in the Johor River basin, Malaysia. *Hydrological Sciences Journal* **60** (5), 873–889.

Thakur, J. K., Khanal, K. & Poudyal, K. 2017 Land cover changes for enhancing water availability in watersheds of Tanahun and Kaski, Nepal. *Journal of Water and Climate Change* **10** (2), 431–448.

Vorosmarty, C. J., McIntyre, P. B., Gessner, M. O., Dudgeon, D., Prusevich, A., Green, P., Glidden, S., Bunn, S. E., Sullivan, C. A., Liermann, C. R. & Davies, P. M. 2010 Global threats to human water security and river biodiversity. *Nature* **467** (7315), 555–561.

Wada, Y., Bierkens, M. F. P., de Roo, A., Dirmeyer, P. A., Famiglietti, J. S., Hanasaki, N., Konar, M., Liu, J., Müller Schmied, H., Oki, T., Pokhrel, Y., Sivapalan, M., Troy, T. J., van Dijk, A. I. J. M., van Emmerik, T., Van Huijgevoort, M. H. J., Van Lanen, H. A. J., Vörösmarty, C. J., Wanders, N. & Wheater, H. 2017 Human–water interface in hydrological modelling: current status and future directions. *Hydrology and Earth System Sciences* **21** (8), 4169–4193.

Wang, R. & Kalin, L. 2018 Combined and synergistic effects of climate change and urbanization on water quality in the Wolf Bay watershed, southern Alabama. *Journal of Environmental Sciences* **64**, 107–121.

First received 25 June 2019; accepted in revised form 22 May 2020. Available online 1 July 2020